Hydrogeol J
DOI 10.1007/s10040-016-1456-1

REPORT

Distinct groundwater recharge sources and geochemical evolution of two adjacent sub-basins in the lower Shule River Basin, northwest China

Liheng Wang[1] · **Yanhui Dong**[1,2] · **Yueqing Xie**[3] · **Fan Song**[1,2] · **Yaqiang Wei**[1,2] · **Jiangyi Zhang**[1,2]

Received: 2 February 2016 / Accepted: 20 July 2016

Abstract Based on analysis of groundwater hydrogeochemical and isotopic data, this study aims to identify the recharge sources and understand geochemical evolution of groundwater along the downstream section of the Shule River, northwest China, including two sub-basins. Groundwater samples from the Tashi sub-basin show markedly depleted stable isotopes compared to those in the Guazhou sub-basin. This difference suggests that groundwater in the Tashi sub-basin mainly originates from meltwater in the Qilian Mountains, while the groundwater in the Guazhou sub-basin may be recharged by seepage of the Shule River water. During the groundwater flow process in the Tashi sub-basin, minerals within the aquifer material (e.g., halite, calcite, dolomite, gypsum) dissolve in groundwater. Mineral dissolution leads to strongly linear relationships between Na^{+} and Cl^{-} and between Mg^{2+}+ Ca^{2+} and $SO_4^{2-} + HCO_3^{-}$, with stoichiometry ratios of approximately 1:1 in both cases. The ion-exchange reaction plays a dominant role in hydrogeochemical evolution of groundwater in the Guazhou sub-basin and causes a good linear relationship between (Mg^{2+}+ Ca^{2+})–($SO_4^{2-} + HCO_3^{-}$) and (Na^{+}+ K^{+})–Cl^{-} with a slope of −0.89 and also results in positive chloroalkaline indices CAI 1 and CAI 2. The scientific results have implications for groundwater management in the downstream section of Shule River. As an important irrigation district in Hexi Corridor, groundwater in the Guazhou sub-basin should be used sustainably and rationally because its recharge source is not as abundant as expected. It is recommended that the surface water should be used efficiently and routinely, while groundwater exploitation should be limited as much as possible.

Keywords Stable isotopes · Hydrochemistry · Groundwater recharge · Arid regions · China

Introduction

Shortage of water resources has become one of the most important challenges to humankind in arid and semi-arid regions (e.g., Western United States, Algeria, Egypt, China and Australia) where rainfall is highly variable and infrequent and evapotranspiration is high (Robertson and Sharp 2013; Eissa et al. 2013; Martos-Rosillo et al. 2014). With a steady growth in population and expanding economic activities, water demand has been increasing and groundwater use has risen dramatically (Zhu et al. 2008; Xi et al. 2010). Poorly regulated groundwater exploitation has created serious consequences such as intense mineralization of groundwater, lowering of the regional water table, land desertification and salinization, deterioration of vegetation and more frequent sand storms (Gonzalez-Ramon et al. 2013). Clearly, the environment will continue to deteriorate without rational exploitation and appropriate management of groundwater.

Sustainable use of groundwater resources in arid and semi-arid areas requires the knowledge of groundwater recharge rates and characteristics; however, it is difficult to estimate recharge using individual conventional methods, such as water balance, lysimeters and numerical simulation (Cloutier

✉ Yanhui Dong
dongyh@mail.iggcas.ac.cn

[1] Key Laboratory of Shale Gas and Geoengineering, Institute of Geology and Geophysics, Chinese Academy of Sciences, P.O. BOX 9825, Beijing 100029, China

[2] University of Chinese Academy of Sciences, Beijing 100049, China

[3] National Centre for Groundwater Research and Training, School of the Environment, Flinders University, Sturt Road, Adelaide 5042, South Australia, Australia

Published online: 06 August 2016

et al. 2006; Negrel et al. 2007; Londono et al. 2008). Recently, methods using environmental isotopes in groundwater, combined with chemistry, have been widely used to investigate various hydrogeological processes (for example origin, movement, mixing, evaporation, groundwater recharge and basin hydrology) to improve understanding of the modern hydrological cycle at local, regional, even global scales (Girmay et al. 2015; Montcoudiol et al. 2015). Chemical and isotopic methods are capable of examining the entire subsurface hydrological cycle and so are likely to infer more reliable conceptual models of groundwater systems, especially in those arid areas with little rainfall and very high potential evaporation (Herczeg and Leaney 2011; Currell and Cartwright 2011).

This study attempted to use stable isotopes and water chemistry to identify the sources of groundwater recharge in Guazhou County (downstream of Shule River Basin) located in the western part of the Hexi Corridor in northwest China (Fig. 1). The Shule River Basin is one of the most water-stressed inland river basins in northwest China because of extreme water deficits with low annual rainfall and high evaporation rates. In the past 20 years, a resettlement project has been planned and implemented by the local government in Gansu Province to develop the Hexi Corridor area (Shule River) and increase food production. Because of the project, irrigated farmland had expanded by 2.8×10^4 ha from 1996 to 2006, and more than 75,000 immigrants had been resettled. Since then, groundwater resources have been increasingly stressed (Ji et al. 2006). Over 70 % of regional water resources have been utilized for irrigating farmland. Over-pumping of groundwater from wells and enhanced water diversion resulted in the decline of hydraulic heads in aquifers at 0.15 m/year from 2000 to 2010 in the middle reach area of the Shule River basin (Huang and Wang 2010). Many springs have been depleted, and the total outflow amount has decreased by 53 % relative to the 1960s in the middle reach area. In addition, some lakes and wetlands have diminished or disappeared along the lower reaches of the Shule River. The groundwater-dependent ecosystem is threatened by falling water tables in the area, and this will also increase the vulnerability of the nearby desert ecosystems. Consequently, there is an urgent need to better understand the recharge sources and circulation of groundwater across the region in order to make a scientifically robust groundwater allocation plan.

Much research about hydrogeology and hydrogeochemical evolution of groundwater has been conducted in other parts of the Hexi Corridor area such as Shiyang River Basin, Zhangye Basin, Jiuquan Basin, Shule River Basin and Dunhuang Basin (Ma et al. 2005, 2013; He et al. 2012, 2015; Wang et al. 2015; Chen et al. 2014). They have shown that the patterns of isotopic compositions and hydrogeochemical data in groundwater are useful to identify recharge sources and to understand the evolution process. There have also been some studies carried out in the Shule River basin, but they focused on the upstream region or gave rough patterns of groundwater circulation of the whole basin (Wang et al. 2015; He et al. 2015). This study aimed to identify groundwater recharge sources in the Guazhou County in the downstream section of Shule River Basin, where groundwater has been more stressed. In addition, based on the hydrogeochemical data, dominant hydrogeochemical processes were characterized using statistical analysis between various ions in groundwater from two different sub-basins. Then, the conceptual groundwater flow model was constructed. The results of this study will provide a better understanding of water resources in the Shule River basin and help the government develop suitable utilization strategies to manage the limited water resources.

Geological and hydrogeological setting of the study area

General setting

The Shule River basin (92.2–99°E, 38–42.6 °N) is located in the western part of Gansu province in northwest China (Fig. 1a) and the total area of the watershed is approximately 41,300 km^2. It consists of the Qilian Paleozoic geosynclinal fold zone in the south, Hexi Corridor alluvial plains in the middle and the Variscan fold belt (the Beishan Mountains) in the north (Fig. 1b). The study area is situated at the downstream section of the Shule River basin, including Guazhou and Tashi sub-basins separated by the Beijie Mountains (Fig. 1c). The Guazhou sub-basin is a piedmont alluvial plain inclined towards west. The elevation ranges between 1,000 and 1,300 m above sea level (MASL). The Tashi sub-basin includes some small intermountain basins and Nanjie Mountains is composed of a series of small individual hills (Fig. 1). Shibao Town, Dongba Town and Tashi Town locate from south to north in this sub-basin. The elevation decreases from 2,000 MASL in the south to 1,500 MASL in the north.

The study area is characterized by a strong continental climate that shows a great variation in temperature and precipitation throughout the year. Temperature typically ranges from −10 to 25 °C, with an annual mean temperature of about 9 °C. Precipitation is approximately 48.2 mm/year. It occurs mainly in the summer and accounts for approximately 70 % of annual precipitation. The annual potential evapotranspiration is around 2,500 mm. As a major tributary of the Shule River, the Tashi River originates from the Qilian Mountains and traverses the Tashi sub-basin from south to north. Its runoff distribution is relatively uniform throughout the year and the average flow rate is about 50 million m^3/year. This river has been dammed by Tashi Dam since 1973 and most water is managed and allocated for an

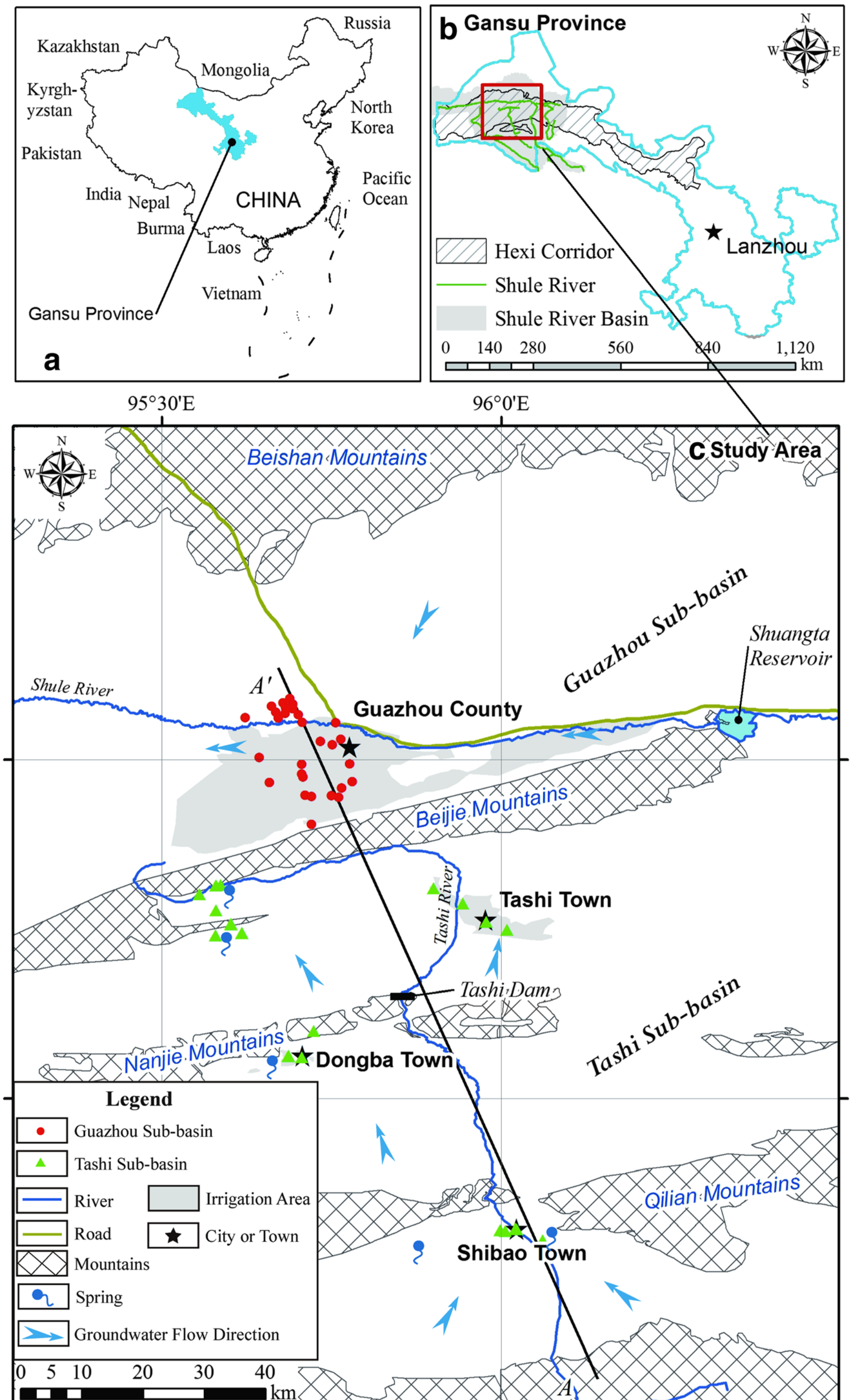

Fig. 1 **a**–**c** Location map of the study area and the sampling sites (the *A*–*A′* line is the location of the cross section in Fig. 2; the *green triangles* represent samples collected from Shibao Town, Dongba Town and Tashi Town from south to north in Tashi sub-basin; the *red* dots represent samples collected from Guazhou sub-basin

irrigation district in the Tashi sub-basin. In addition, the Shule River flowed from east to west through the Guazhou sub-basin before the establishment of the Shuangta Reservior in 1958. More than three quarters of the Shule River water was used for irrigation in the Guazhou sub-basin after building the dam (data from Hydrological Bureau in the Gansu province, China).

Geology and hydrogeology

The study area consists of two geological units, including the southern Qilian Palaeozoic geosynclinal fold zone and the Hexi Corridor depression. The uplift of the Qilian Mountains in the south has occurred since the end of the Palaeozoic, and has formed an active fold and thrust-belt that extends along the north-eastern margin of the Tibetan Plateau. During the end of the Palaeozoic and throughout the Mesozoic era, the embryonic form of the Hexi Corridor was created (Gansu Geology Survey 1978). A series of north-east east (NEE) tectonic activity has cut the Hexi Corridor into two parts: the Guazhou sub-basin and the Tashi sub-basin.

The mountains, including Qilian Mountains, Nanjie Mountains and Beijie Mountains, are composed of Archean and Sinian metamorphic and igneous rocks. The main lithology includes gneiss, schist, marble, tuff and granite. The intensive denudation and erosion has continued for millions of years owing to the ongoing uplift of the mountains. The loose clastic materials are then carried down during surface runoff to form the sediment of the basins.

In the Tashi sub-basin, the diluvial and proluvial aquifer is formed from highly permeable cobble and gravel deposits that are between 100 and 300 m thick constituting one unconfined aquifer layer. The groundwater depth ranges between 0 and 150 m below the land surface (Fig. 2). The well yield is about 3,000–50,000 m^3/day, and the hydraulic gradient ranges from 3 to 10 ‰ (Gansu Geology Survey 1978). The highly permeable deposits, particularly in piedmont fans, allow surface runoff to seep down and recharge the aquifer quickly. As mentioned in the preceding, Nanjie Mountain has a series of small individual hills (Fig. 1), which block some parts of groundwater flow and some springs can be found in front of the hills (Fig. 2); however, the permeable unconsolidated sediments around these hills allow groundwater to flow in them from south to north. This ensures that the whole gravel aquifer in the Tashi sub-basin is a continuous flow system and the groundwater flow direction is mainly from south to north.

The aquifer in the Guazhou sub-basin is composed of interbedded coarse sand, fine sands and clay loams that form a multilayer aquifer, and so the average grain size in the aquifer is finer than that in the Tashi sub-basin (Gansu Geology Survey 1978). The thickness of this aquifer is between 25 and 70 m. The water table is about 17–50 m below the land surface, and the top of the confined aquifer is 21–50 m below the surface. From east to west, the well yield decreases from about 4,000 to 700 m^3/day. Groundwater in this sub-basin is recharged by lateral flow, canal system seepage, and farmland irrigation water seepage. It discharges mainly via evapotranspiration and artificial abstraction. The overall groundwater flow in the Guazhou sub-basin is generally from east to west (Fig. 1).

Materials and methods

In this study, geochemicals and stable isotopes were analyzed to determine the major sources of these two adjacent sub-basins. In total, 53 samples were collected from July 2012 to July 2014 with 24 samples in the Tashi sub-basin and 29 samples in the Guazhou sub-basin. The location of sampling sites is shown in Fig. 1. A submersible pump was used to collect samples from wells. Before sampling, each well was pumped continuously for at least three well volumes to ensure that samples were representative of the groundwater. The spring water was sampled at the discharge point in order to minimize possible isotopic fractionation and geochemical reaction. All samples were filtered through 0.45-μm membrane filters and kept in airtight HDPE bottles. All the bottles were washed three times using the filtered water before sample collection. For each sampling site, five bottles of water were collected. Two bottles were acidified by adding 1 % HNO_3 to produce a pH of around 1.5 in order to determine the major cations. The other three bottles were used for anion and stable isotope analysis. All samples were stored below 4 °C until analysis.

Temperature, pH, total dissolved solids (TDS), electrical conductance (EC) and total alkalinity (as HCO_3^-) by titration were monitored in the field. Cations and anions were analyzed at the Key Laboratory of Shale Gas and Geoengineering, Institute of Geology and Geophysics, Chinese Academy of

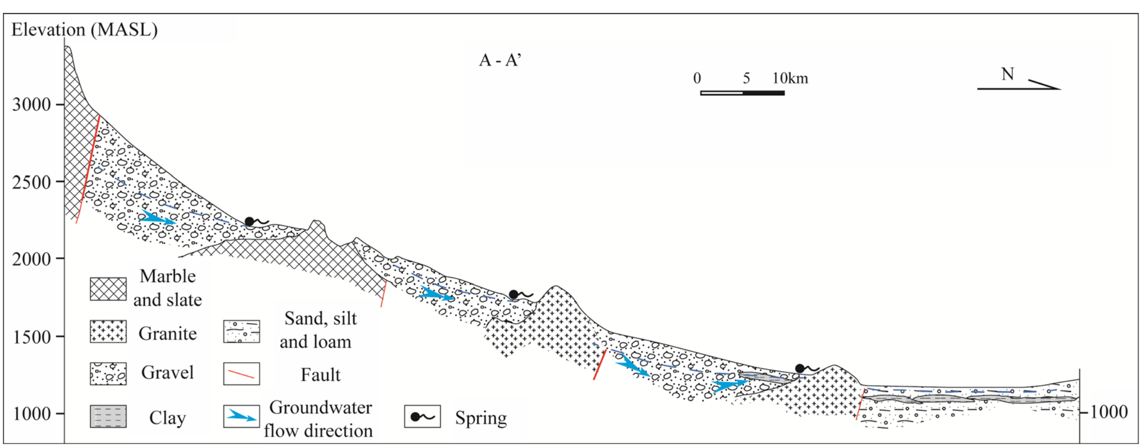

Fig. 2 Hydrogeological cross-section of the study area from the Qilian Mountain to the Guazhou sub-basin (modified from Gansu Geology Survey 1978). *MASL* meters above sea level

Science (CAS). Major anions (Cl^-, SO_4^{2-}, NO_3^-) were measured using ion chromatography (IC), while major cations and trace elements were analyzed using inductively coupled plasma mass spectrometry (ICP-MS; Agilent Technologies, California, USA). Calibrations for cation analyses were performed using appropriately diluted standards and both laboratory and international reference materials were used as checks for accuracy. Instrumental drift during ICP-MS analysis was corrected using In and Pt internal standards. Analytical errors were within 3 % of concentrations based on reproducibility of samples, and the detection limit was 0.1 mg/L for undiluted samples. An internal check on the quality of chemical data was made by determining the ionic balance which was less than 5 %.

Stable isotopes (^2H or D and ^{18}O) were analyzed by using a laser spectrometry DLT-100 Liquid-Water isotope analyzer, automated injection designed by Los Gatos Research at the Key Laboratory of Water Cycle and Related Land Surface Processes, Institute of Geographic Sciences and Natural Resources Research, CAS. The results were expressed as δ (‰), defined by:

$$\delta = \left(\frac{R_s - R_P}{R_P}\right) \times 1,000 \quad (1)$$

where δ is the isotopic deviation in ‰, R_s is the isotopic ratio ($D/^1H$, $^{18}O/^{16}O$) of the sample and R_P is the isotopic ratio of the international reference. All δ values of water samples are conventionally reported relative to the international standard VSMOW (Vienna standard mean ocean water). The analytical errors were 0.1 and 1 ‰ for $\delta^{18}O$ and δD, respectively. The analysis results of the isotopic composition of water and hydrogeochemical data are shown in Table 1.The geochemical code PHREEQC was used to evaluate speciation and saturation indices (SI; Parkhurst and Appelo 1999). Range, mean values and standard deviations of the SI for common minerals are shown in Table 2.

Results

Stable isotope compositions

The isotopic and geochemical results are shown in Table 1, including the site information, well depth, basic physical and chemical data for groundwater. Samples are arranged in the geographic order (from south to north) in the table.

Although the water samples were collected in July and November, their isotopic compositions were so similar that they can be treated as a whole (Table 1). The $\delta^{18}O$ and δD values of groundwater samples collected in the vicinity of the Qilian Mountains is about −11.7 and −81 ‰, respectively. The values gradually increased towards the north, from −11.6 to −10.4 ‰ for $\delta^{18}O$, and from −79 to −72 ‰ for δD, respectively (Table 1), which is consistent with the groundwater flow direction in the Tashi sub-basin. Meanwhile, the mean $\delta^{18}O$ and δD values of the groundwater in this sub-basin are −11.1 and −77 ‰, respectively. In contrast, groundwater from the Guazhou sub-basin is significantly enriched in heavy isotopes compared to that of Tashi. The $\delta^{18}O$ and δD compositions range from −9.2 to −7.6 ‰ and −61 to −51 ‰, with mean values of −8.1 and −55 ‰, respectively (Table 1).

Hydrogeochemistry of groundwater

In the Tashi sub-basin, the total dissolved solids (TDS) in groundwater ranged from 371.0 to 2,270.0 mg/L, with a mean concentration of 2,084.9 mg/L. The pH value ranged from 7.0 to 8.3 and the mean temperature of groundwater was 11.8 °C. Moving from south to north, along the groundwater flow direction, the overall chemistry of the anion facies in the groundwater types changed from HCO_3^--dominated to SO_4^{2-}, and then to no-dominant-anions (Fig. 3). Magnesium, the most abundant of the cations, varied between 30.58 and 208.81 mg/L in groundwater, and corresponding milliequivalents is 2.55–17.4 meq/L. It accounted for more than 50 % of total cations in most samples. So Mg^{2+} is the predominant cation and the groundwater in Tashi sub-basin is of the Mg^{2+} type.

In the Guazhou sub-basin, all of the samples were collected from wells. They had a narrow temperature range (11.0–13.5 °C), with similar pH values (7.1–8.1), and TDS values ranged from 449 to 3,130 mg/L (mean of 1,506.8 mg/L). Compared to the groundwater samples collected from the Tashi sub-basin, Ca^{2+}, Cl^-, SO_4^{2-}, and NO_3^- concentrations in groundwater from Guazhou sub-basin were higher obviously. Cl^- (mean value 318.1 mg/L) and SO_4^{2-} (mean value 477.9 mg/L) are the most abundant anions, and Na^+ is the most abundant cation, whose values vary between 39.4 and 402.0 mg/L; therefore, most of the groundwater samples from the Guazhou area are of the SO_4^{2-}–Cl^-–Na^+ type (Fig. 3).

Discussion

Groundwater recharge

In most cases, precipitation is a predominant recharge source for groundwater systems. Before becoming rainfall, the water vapour undergoes isotope fractionations during transportation process from ocean to continent. During the process, δD and $\delta^{18}O$ in rainwater are correlated very well with $\delta D = 8\delta^{18}O + 10$. It is well known as the global meteoric water line (Craig 1961). In addition, the isotopic composition of rainfall can be empirically correlated to a number of factors or effects, including altitude, latitude, season, temperature and rainfall amount.

Table 1 Major ions and isotopic compositions of groundwater samples in the study area, locations of which are shown in Fig. 1

Sample ID	Well depth	Temp. (°C)	pH	TDS (mg/L)	EC (μS/cm)	Na^+ (mg/L)	K^+ (mg/L)	Ca^{2+} (mg/L)	Mg^{2+} (mg/L)	Cl^- (mg/L)	SO_4^{2-} (mg/L)	HCO_3^- (mg/L)	NO_3^- (mg/L)	D (‰)	^{18}O (‰)	Date (year. month)
TS01	30 m	5.2	7.8	371.0	529	26.9	2.5	25.0	34.8	22.7	43.3	225.8	0.64	−85	−12.5	2013.11
TS02	Spring	7.5	7.5	375.3	1,485	31.9	2.3	29.1	30.6	20.2	20.8	262.4	0.17	−79	−11.7	2013.11
TS03	Spring	9.4	7.0	411.0	1,605	25.3	2.4	42.9	33.1	17.4	50.0	242.0	0.23	−82	−11.7	2013.11
TS04	Spring	14.4	7.4	463.3	1,831	35.8	2.5	30.3	40.1	32.5	54.0	235.9	0.30	−79	−10.9	2013.11
TS05	Spring	12.5	8.25	290	488	32.6	2.5	30.6	29.7	43.3	92.0	175.7	0.99	–	–	2013.11
TS06	45 m	14.5	8.2	660.0	928	60.6	2.5	33.2	61.6	70.8	281.3	126.9	0.99	−77	−11.8	2012.7
TS07	60 m	13.0	7.8	570.0	772	26.1	3.2	59.7	52.8	19.1	71.2	368.5	1.02	–	–	2014.7
TS08	Spring	14.0	8.2	724.0	1,039	97.7	2.2	38.8	59.6	157.7	279.2	73.2	2.60	−80	−11.5	2012.7
TS09	Spring	11.6	8.3	724.0	710	117.0	5.5	48.4	83.2	159.3	254.6	351.5	0.94	−79	−12.0	2014.11
TS10	Spring	12.5	7.5	1,240.0	1,932	168.0	9.0	74.5	112.0	143.4	367.3	432.2	1.22	–	–	2014.7
TS11	Spring	12.5	7.7	1,206.0	1,873	199.0	8.5	52.8	70.3	227.9	503.1	87.9	0.84	−80	−11.1	2014.7
TS12	Spring	9.5	7.9	719.0	1,006	62.9	5.4	48.1	71.2	56.0	72.0	431.0	0.45	−75	−11.1	2013.11
TS13	Spring	9.5	7.6	752.0	1,079	66.8	5.6	54.1	73.3	58.9	73.5	463.8	0.49	−75	−11.0	2013.11
TS14	Spring	11.4	7.7	821.0	1,204	63.8	7.6	53.3	85.0	51.6	137.5	451.5	0.33	−77	−10.9	2013.11
TS15	Spring	14.4	7.4	2,270.0	3,500	361.1	13.1	96.2	208.8	664.7	420.9	457.7	0.69	−77	−10.6	2013.11
TS16	Spring	13.4	7.6	1,492.0	2,310	191.5	8.6	68.7	143.6	373.3	236.1	381.7	0.76	−76	−10.6	2013.11
TS17	Spring	13.0	7.5	1,476.0	2,560	208.8	8.6	65.7	145.9	397.6	262.1	363.9	0.77	−75	−10.5	2013.11
TS18	Spring	12.3	7.4	1,851.0	3,110	388.8	11.3	94.6	132.0	543.9	352.1	433.2	0.61	−75	−10.5	2013.11
TS19	Spring	11.0	7.6	1,749.0	3,430	314.0	12.3	85.4	190.0	521.1	781.6	406.4	0.73	−79	−10.7	2013.11
TS20	Spring	14.5	7.7	1,670.0	2,676	124.0	8.9	50.1	114.0	103.6	352.5	347.8	0.79	–	–	2014.7
TS21	45 m	11.0	8.0	1,108.0	1,703	125.0		46.4	97.1	168.6	542.2	87.9	4.14	−75	−10.5	2014.7
TS22	80 m	12.7	7.4	1,596.0	2,280	191.4	7.0	75.4	145.5	213.0	328.4	572.2	4.69	−70	−10.2	2013.11
TS23	65 m	12.8	7.4	2,040.0	3,170	296.7	9.4	65.0	184.8	299.3	556.8	551.5	3.63	−71	−10.6	2013.11
TS24	35 m	10.5	7.6	1,180.0	1,828	148.0	7.3	79.7	102.0	104.7	324.9	461.2	1.90	–	–	2014.7
GZ01	55 m	11.0	7.8	2,240.0	3,662	213.0	3.7	132.0	166.0	359.5	792.0	368.6	7.70	−54	−7.9	2012.7
GZ02	30 m	12.5	8.0	2,140.0	3,489	238.0	5.8	123.0	119.0	301.4	831.2	165.3	7.86	−53	−7.8	2012.7
GZ03	65 m	12.0	8.1	1,160.0	1,793	146.0	2.6	64.9	84.9	247.1	408.0	170.4	4.69	−54	−7.8	2014.7
GZ04	55 m	12.0	7.8	1,382.0	2,177	169.0	3.1	87.5	102.0	340.9	481.0	141.1	6.04	−54	−8.0	2014.7
GZ05	50 m	11.5	7.8	967.0	1,459	87.9	1.5	58.3	62.9	144.4	307.5	164.8	2.42	−55	−8.3	2014.7
GZ06	50 m	13.0	7.8	2,980.0	4,943	324.0	7.9	171.0	126.0	658.6	803.5	92.3	11.75	−56	−8.1	2014.7
GZ07	40 m	12.0	7.9	2,760.0	4,562	326.0	5.8	155.0	116.0	603.1	787.2	106.5	7.50	−57	−9.2	2014.7
GZ08	80 m	13.0	7.9	2,110.0	3,437	244.0	4.4	117.0	120.0	334.3	872.6	125.0	3.49	−57	−9.2	2014.7
GZ09	40 m	13.0	7.8	1,572.0	2,506	187.0	3.6	74.5	60.2	304.0	421.4	87.9	2.30	−61	−8.1	2014.7
GZ10	80 m	12.1	7.5	1,541.0	2,650	256.5	9.2	91.7	121.1	397.4	295.2	389.5	2.42	−51	−7.6	2013.11
GZ11	45 m	12.0	7.4	1,973.0	2,970	253.6	10.5	133.3	170.1	449.8	430.3	487.8	2.45	−54	−8.1	2013.11
GZ12	65 m	12.3	7.5	1,439.0	2,390	222.3	8.7	85.1	116.5	338.4	275.3	405.1	1.57	−56	−8.4	2013.11
GZ13	40 m	12.7	7.6	952.0	1,466	126.3	7.2	55.0	82.0	111.7	146.4	482.9	2.07	−55	−8.1	2013.11
GZ14	65 m	12.2	7.4	1,202.0	1,741	160.5	9.4	75.7	102.6	189.2	201.4	522.7	4.28	−53	−7.6	2013.11
GZ15	35 m	13.5	7.1	3,130.0	5,203	402.0	21.8	204.0	250.0	420.7	1131.3	567.5	9.62	–	–	2014.7
GZ16	65 m	13.0	7.3	1,860.0	3,005	212.0	15.8	116.0	127.0	162.8	563.6	442.7	4.35	–	–	2014.7
GZ17	25 m	13.0	7.6	1,114.0	1,714	264.0	4.6	74.8	22.0	301.2	403.0	73.2	6.55	–	–	2014.7
GZ18	25 m	12.5	7.5	996.0	1,509	226.0	5.5	71.7	22.8	278.9	363.1	97.6	6.16	–	–	2014.7
GZ19	20 m	12.0	7.7	991.0	1,501	253.0	4.5	67.1	22.7	316.5	380.2	72.5	5.72	–	–	2014.7
GZ20	20 m	12.0	7.8	1,146.0	1,769	269.0	4.9	76.1	23.0	308.6	433.9	97.6	5.75	–	–	2014.7
GZ21	20 m	11.6	7.7	1,418.0	2,240	273.0	4.8	84.7	23.3	390.2	406.6	27.6	5.85	–	–	2014.7
GZ22	20 m	11.0	7.5	1,323.0	2,075	297.0	7.3	92.7	32.5	367.8	405.6	92.5	5.96	–	–	2014.7
GZ23	15 m	11.5	7.3	1,395.0	2,200	356.0	6.3	93.7	33.3	410.1	557.5	97.6	6.32	–	–	2014.7

Table 1 (continued)

Sample ID	Well depth	Temp. (°C)	pH	TDS (mg/L)	EC (μS/cm)	Na^+ (mg/L)	K^+ (mg/L)	Ca^{2+} (mg/L)	Mg^{2+} (mg/L)	Cl^- (mg/L)	SO_4^{2-} (mg/L)	HCO_3^- (mg/L)	NO_3^- (mg/L)	D (‰)	^{18}O (‰)	Date (year. month)
GZ24	20 m	12.0	7.7	932.0	1,399	186.0	3.4	79.0	30.7	288.4	366.3	27.6	5.83	–	–	2014.7
GZ25	35 m	12.0	7.7	1,311.0	2,054	279.0	4.9	104.8	36.7	355.4	498.4	97.6	6.80	–	–	2014.7
GZ26	45 m	13.5	8.0	492.0	637	49.3	0.9	36.4	36.0	65.9	178.1	107.4	0.72	–	–	2014.7
GZ27	30 m	12.0	8.0	449.0	563	39.4	0.7	37.9	46.8	60.3	185.6	117.2	0.88	−53	−8.0	2014.7
GZ28	35 m	13.0	7.9	1,071.0	1,639	199.0	4.9	61.6	40.4	264.5	359.2	112.3	5.50	–	–	2014.7
GZ29	15 m	12.5	7.7	1,652.0	2,645	360.0	6.4	134.0	40.2	455.1	573.4	170.9	6.71	–	–	2014.7

Because of the geographic characteristics of the Hexi Corridor, the isotopic composition of rainfall may differ between the Qilian Mountains and the plains zone. As a result, the source and circulation history of groundwater can be deciphered by comparing the isotopes (D and ^{18}O) of rainfall and groundwater.

Zhao et al. (2011) defined the Yeniugou local meteoric water line (LMWL) as $\delta D = 7.6\delta^{18}O + 12.4$ ($R^2 = 0.99$). The Yeniugou station is located at an elevation of 3,320 m in the Qilian Mountains and lies 380 km southeast of the study area. Its latitude and longitude are 99°38′E, 38°42′N respectively. At this site, the mean annual precipitation and temperature were 401.4 mm and −3.1 °C. This LMWL can represent the isotopic characteristics of precipitation at high altitudes in the Qilian Mountains. Since there are no long-term data on isotopic ratios in the Shule River Basin, data from the Zhangye Meteorological Station was chosen. This station is located 430 km southeast of the Guazhou county (100°26′E, 38°55′N, 1,480 m elevation) and has been one of the members of the International Atomic Energy Agency (IAEA) network since 1985. At this site, the mean annual precipitation and temperature are 118.12 mm and 7.59 °C, respectively. The LMWL for the Zhangye station is $\delta D = 7.5\delta^{18}O + 2.7$ according to the International Atomic Energy Agency database (IAEA and WMO 2004). This LMWL can represent the relationship between $\delta^{18}O$ and δD in the plains region of the Hexi Corridor and it has been applied in many studies (Ma et al. 2005, 2013; He et al. 2012, 2015). The intercept of the Yeniugou LMWL was slightly higher than that of the Zhangye LMWL, indicating more moist and weaker evaporative conditions in the mountains. In addition, the surface water collected from Shuangta Reservoir to Guazhou county represent the characteristics of lower reaches of Shule River water. The $\delta^{18}O$ and δD values have been shown in previous studies (Wang et al. 2015; He et al. 2015). The $\delta^{18}O$ and δD compositions range from −9.1 to −6.9 ‰ and −56 to −49 ‰, with average values of −8.2 and −53 ‰, respectively.

Table 2 Descriptive statistics for saturation indices of groundwater in the study area. Values were calculated using the PHREEQC software. *SD* standard deviation

Mineral	Tashi sub-basin				Guazhou sub-basin			
	Min	Max	Mean	SD	Min	Max	Mean	SD
Anhydrite	−2.85	−1.29	−1.87	0.41	−1.96	−0.87	−1.40	0.28
Aragonite	−0.76	0.64	−0.02	0.33	−0.84	0.31	−0.15	0.33
Calcite	−0.61	0.79	0.14	0.33	−0.69	0.46	0.01	0.33
Dolomite	−1.22	1.99	0.63	0.72	−1.77	1.08	0.03	0.88
Gypsum	−2.59	−1.03	−1.61	0.41	−1.71	−0.61	−1.15	0.28
Halite	−7.90	−5.26	−6.51	0.84	−7.18	−5.30	−5.85	0.46

During surface runoff and the groundwater recharge process, isotopic fractionation will enrich heavy stable isotopes and retain the linear relationship between δD and $\delta^{18}O$. Generally speaking, groundwater samples fell below or along the LMWL if they have closed relation with these groundwater. Figure 4 shows the δD and $\delta^{18}O$ values in the groundwater and surface water from the study area in relation to the meteoric water lines.

Most groundwater samples collected in Tashi are distributed below the Yeniugou LMWL but above the Zhangye LMWL, indicating that there is a close relationship between the groundwater in Tashi and the precipitation in the Qilian Mountains. The annual weighted mean values of δD and $\delta^{18}O$ at Yeniugou were −40 and −6.3 ‰ and the winter weighted mean values of δD and $\delta^{18}O$ were −118 and −16.6 ‰, respectively (Zhao et al. 2011). It seems that winter precipitation is a major recharge source of the groundwater because all of the groundwater samples were strongly depleted compared with that of the annual weighted mean values; however, in winter, the precipitation is mainly snow instead of rain, so it is difficult to recharge groundwater directly.

The plot of δD and $\delta^{18}O$ shows a good linear relationship that followed the evaporation line: $\delta D = 4.5\delta^{18}O - 27.1$ ($R^2 = 0.64$, Fig. 4). Meanwhile, the mean isotopic values of snow and ice-melt water that was collected from Qilian Mountains (located 54 km southeast of the Shibao Town, 39°30.1′N 96°30.8′E, 4,214 m elevation) during the thawing period (from June to October, 2012–2013) were −86 ‰ δD and −13.1 ‰ $\delta^{18}O$, respectively (Wang et al. 2016). It falls exactly on the intersection of the Yniugou LMWL and the evaporation line of groundwater in Tashi (pentagram in

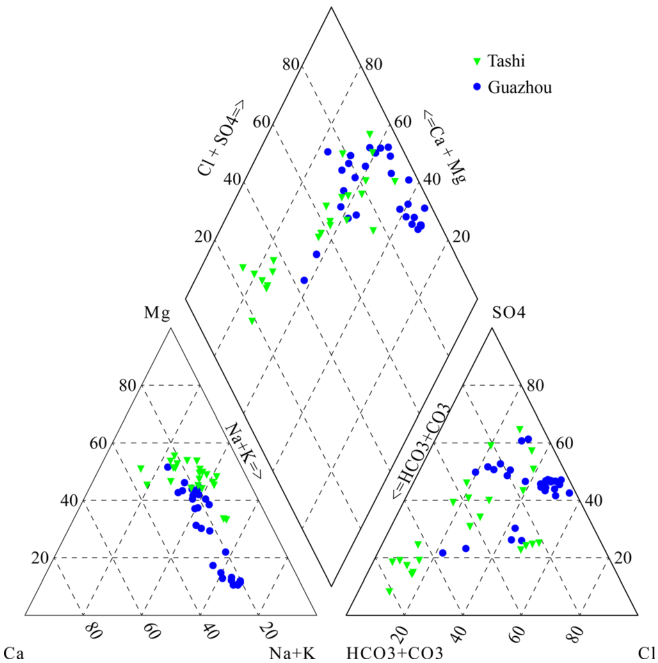

Fig. 3 Trilinear diagram illustrating the chemical composition of groundwater in the study area

Fig. 4). Undoubtedly, the snow and ice-melt water in Qilian Mountains is a major recharge source of the groundwater in Tashi.

In addition, although the isotopic values of groundwater in the Tashi sub-basin were more negative on the whole, it is noticed that heavy isotopes of groundwater samples in Tashi were enriched along the groundwater flow direction. For example, the $\delta^{18}O$ values were −12.0, −11.6, and −10.7 ‰ from south to north (Fig. 4). This phenomenon is often found in arid areas such as northwest China and Australia (Wang et al. 2015; Dogramaci and Skrzypek 2015) and has been attributed to evaporative effect; therefore, it indicates that less evaporation has occurred along the groundwater flow direction from south to north in the Tashi sub-basin.

The isotopic ratios of the groundwater from Guazhou were also between Yeniugou LMWL and Zhangye LMWL (Fig. 4). These were similar to those from Tashi but the difference was that the δD and $\delta^{18}O$ values were more positive. It indicates that more intensive evaporation occurs in Guazhou or the groundwater origins are different from Tashi. It is necessary to analyze the isotopes of irrigation water because the Guazhou sub-basin is one of the most important agricultural irrigation areas in Hexi Corridor. Shule River water is the only source of irrigation water in Guahzou sub-basin; some isotopic data of Shule River water, collected from Shuangta Reservoir during previous studies (Wang et al. 2015; He et al. 2015), are shown in Fig. 4 using square symbols. It is noted that groundwater δD and $\delta^{18}O$ values of Guazhou are distributed close to those values associated with the surface water and they overlap each other, indicating that there is a very close relationship between them.

In addition, the weighted average isotopic values of rainfall at the Zhangye station were −27 ‰ for δD and −3.5 ‰ for $\delta^{18}O$ in the summer. In comparison, these isotopic values were −118 ‰ for δD and −16.6 ‰ for $\delta^{18}O$ in the winter (IAEA and WMO 2004). The isotopic values of rainfall in summer are more positive than the values for all of the groundwater samples, and the summer precipitation accounts for more than 70 % of annual precipitation while winter is only 6 %. Moreover, Edmunds et al. (2006) used the Cl^- mass balance method to calculate an average direct local rainwater recharge rate of around 0.95–3 mm/year in the nearby Minqin Basin with an annual rainfall of 89–120 mm. As geographical and hydrogeological conditions are similar between Minqin Basin and Shule Basin, it is expected that direct groundwater recharge from rainfall in the study area is much less than 1 mm/year because of more scarce rainfall (Wang et al. 2015). Similar findings have been reported in adjacent areas, for example, Jinchang Basin, Dunhuang Basin and Jiuquan Basin (Ma et al. 2010, 2013; He et al. 2012). Combining the

Fig. 4 Plot of δD and $\delta^{18}O$ for Shule River water and groundwater in the study area. (*Blue*, *yellow*, *green*, representing the southern, central and northern Tashi sub-basin, respectively)

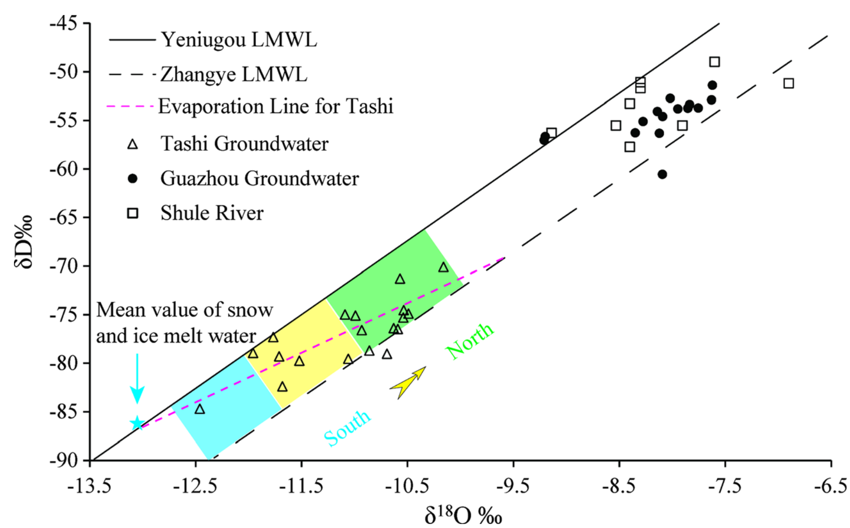

evidences of isotopes and Cl^- mass balance, precipitation in the plains does not contribute greatly to the recharge of groundwater. In summary, Shule River water is a main recharge source of groundwater in Guazhou sub-basin, rather than precipitation in the plains.

Groundwater geochemical characteristics and evolution

The principal characteristics of the groundwater in the study area are low alkalinity (mean value 7.67, Table 1) and relatively high TDS (mean value 1.3 g/L). Despite the high TDS, the groundwater in the study area is good in quality compared to other arid regions (Herczeg et al. 2001; Sun et al. 2016). In many arid regions across the world, a high evaporation rate and a low rainfall usually encourage groundwater salinization, and hence evaporation is often a significant control factor on groundwater quality. Overall, concentrations of many groundwater ions increased evidently with increasing TDS in the study area, suggesting the progressive build-up of salt. In groundwater samples collected from the Tashi sub-basin, Mg^{2+}, Na^+, and Cl^- concentrations correlated with TDS and the coefficients of correlation (R^2) are 0.91, 0.86 and 0.73 respectively (Fig. 5a); however, in the Guazhou sub-basin, a strongly linear relationship was found between Ca^{2+} and TDS ($R^2 = 0.92$) and between SO_4^{2-} and TDS ($R^2 = 0.78$) respectively (Fig. 6a). Generally, the groundwater TDS of the Guazhou sub-basin is higher than that of the Tashi sub-basin, with mean concentrations of 1.5 and 1.0 g/L respectively. These differences indicate that different hydrogeochemical evolutionary routes occur in the two sub-basins and these two sub-basins have different sources of groundwater recharge.

In the Tashi sub-basin, the dominant anion species in groundwater changes systematically from HCO_3^-, SO_4^{2-} to Cl^- to no dominant ion along the groundwater flow direction from south to north. This phenomenon has been observed in many arid areas such as the northern Sahara sedimentary basin, Algeria (Guendouz et al. 2003), as well as other inland river basins in northwestern China (Wang et al. 2015; Ma et al. 2013). Because the chemical species dissolved in the groundwater are not independent of each other, relationships between different ions can be used to study the characteristics and mineralization sources of the groundwater. Generally, the Cl^- ion can be used as a conservative reference element to study water–rock interaction because it undergoes very limited chemical and biological reactions in a natural environment (Edmunds et al. 2003). The mean values of Cl^- are 22.4, 110 and 273.6 mg/L in the vicinity of the Shibao Town, the south Nanjie Mountains, and the north Nanjie Mountains, respectively, in the Tashi sub-basin. This shows that Cl^- increases continuously along the groundwater flow path and its concentration is affected by evaporation, because Cl^- mainly originates from the dissolution of halite in evaporative deposits, and its concentration increases when intense evaporation occurs along the flow path.

In addition, a good linear relationship was found between Na^+ and Cl^- for the groundwater samples in the Tashi sub-basin: $Na^+ = 0.86\ Cl^- + 1.6$ ($R^2 = 0.89$, Fig. 5b). This suggests that the dissolution of halite has considerable control on the Na^+ and Cl^- concentrations. The SI of halite for all samples was far less than 0 (Table 2), indicating that the halite can dissolve into groundwater either in the recharge area or the discharge area. A significant feature is that the mNa^+/Cl^- (molar) ratio is greater than 1 for most samples, and the mean

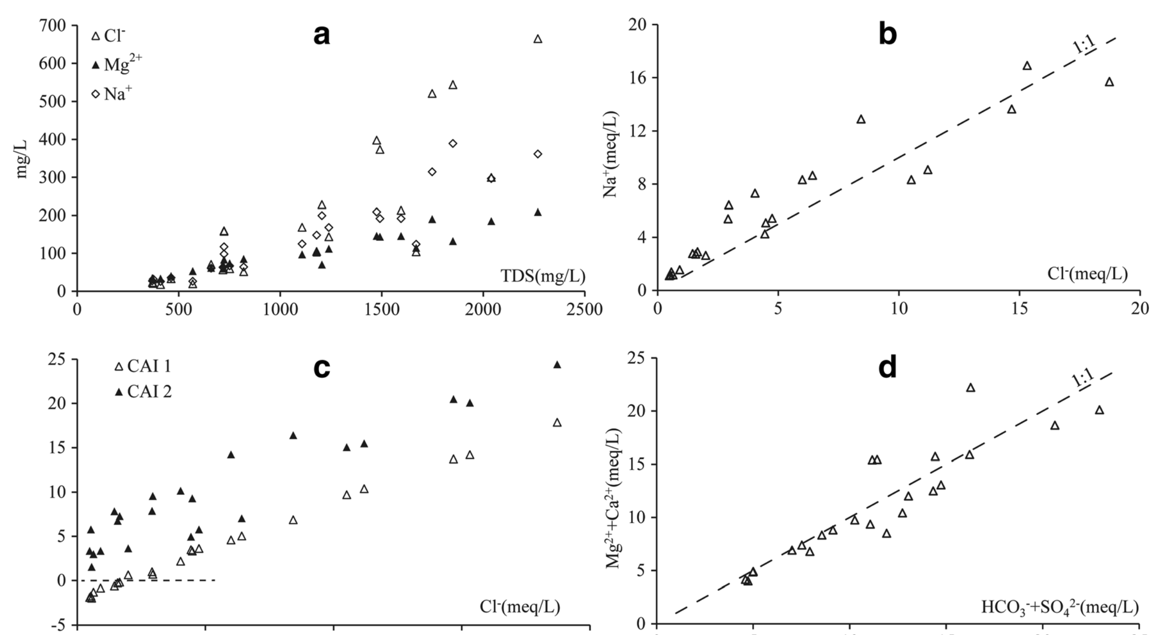

Fig. 5 **a**–**d** Relationships between various groundwater chemical species in the Tashi sub-basin

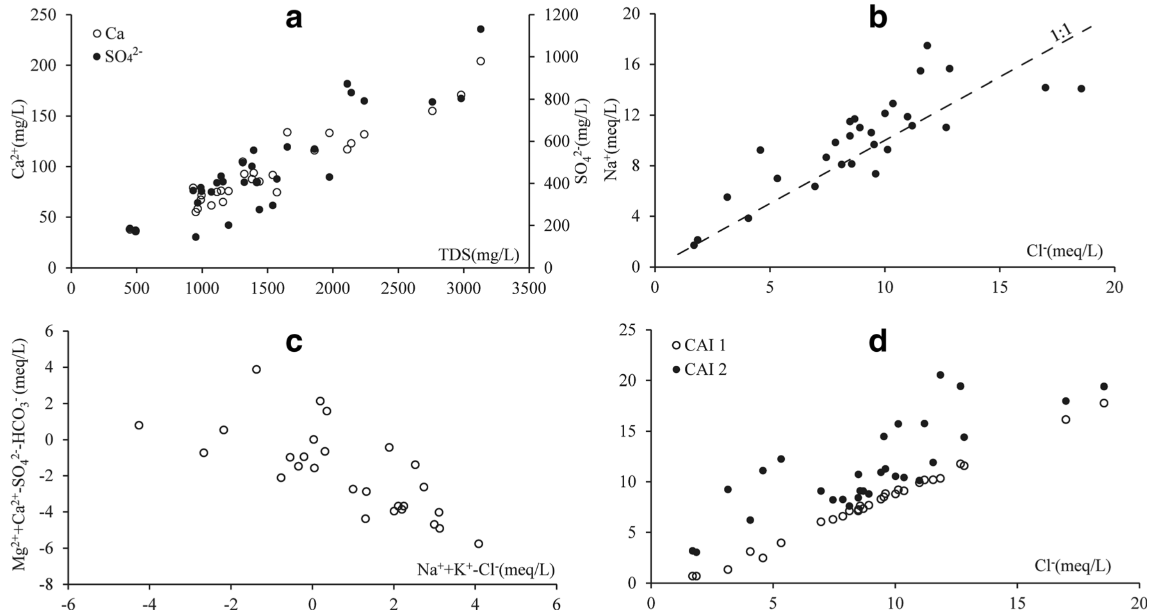

Fig. 6 **a**–**d** Relationships between various groundwater chemical species in the Guazhou sub-basin

value is 1.54 in the Tashi sub-basin. This is indicative of mineral dissolution or ion exchange. Schoeller (1965) defined two chloroalkaline indices CAI 1 and CAI 2, which can be used to determine the effect of ion exchange:

$$\begin{cases} \mathrm{CAI\,1} = \mathrm{Cl^-}\text{-}[(Na^+ + K^+)/\mathrm{Cl^-}] \\ \mathrm{CAI\,2} = \mathrm{Cl^-}\text{-}\left[(Na^+ + K^+)/\mathrm{SO_4^{2-}}\right] + \mathrm{HCO_3^-} + \mathrm{CO_3^{2-}} + \mathrm{NO_3^-} \end{cases} \quad (2)$$

When there is an exchange between Ca^{2+} or Mg^{2+} in the groundwater with Na^+ and K^+ in the aquifer, both the CAI 1 and CAI 2 indices are negative, and if there is a reverse ion exchange, then both these indices will be positive (Schoeller 1965). The values of CAI 1 and CAI 2 in the Tashi sub-basin vary with TDS, and they are positive in relatively high-salinity groundwater but a few samples show negative values of CAI 1 in low-salt water (Fig. 5c), which indicates that reverse ion exchange is the dominant process in the groundwater and chloroalkaline is in disequilibrium in low-salt water.

An additional significant characteristic of the groundwater samples from the Tashi sub-basin is that the plot of Mg^{2+}+ Ca^{2+} versus $SO_4^{2-} + HCO_3^-$ shows a good linear relationship that followed the expected 1:1 stoichiometry ratio (Fig. 5d, $R^2 = 0.82$), although a few points were slightly below the 1:1 line, indicating that Mg^{2+}, Ca^{2+}, SO_4^{2-}, and HCO_3^- were derived from a mixture of the dissolution of calcite, dolomite and gypsum in this sub-basin. Moreover, the values of the mMg^{2+}/Ca^{2+} ratio range between 1.29 and 4.74 with the mean value of 2.72, which is consistent with the abundant Mg-rich lithology of the Tashi sub-basin. Clearly, dissolution of minerals in aquifers is a major control factor during the groundwater flow process in the Tashi sub-basin, also leading to the gradual increase in the SI of some minerals from the recharge area to the discharge area and the mean SI values of calcite and dolomite are slightly greater than 0.

In the Guazhou sub-basin, most samples were the $SO_4^{2-} + Cl^-$ type (Fig. 3). For the cations, Na^+ and Mg^{2+} were dominant ions in the southern part of the sub-basin, but Na^+ was the only dominant cation in the northern part. Similar to Tashi sub-basin, a linear relationship was also found between Na^+ and Cl^- (Fig. 6b, $R^2 = 0.69$) and the mNa^+/Cl^- is about 1.15. However, the plot of Mg^{2+}+ Ca^{2+} versus $SO_4^{2-} + HCO_3^-$ does not show a linear relationship, indicating that these ions were not derived from simple dissolution of calcite, dolomite and gypsum. The mean value of $(Mg^{2+}+ Ca^{2+})/(SO_4^{2-} + HCO_3^-)$ is about 0.84, indicating a deficiency in cations. The excess negative charge must be balanced by Na^+; meanwhile, a linear relationship between Na^+ and SO_4^{2-} was found ($R^2 = 0.45$), indicating the dissolution of mirabilite is also a main process to control the Na^+ and SO_4^{2-}.

Moreover, the evolution of salinity in the groundwater was also explored using a plot of $(Mg^{2+}+ Ca^{2+})–(SO_4^{2-} + HCO_3^-)$ versus $(Na^+ + K^+)–Cl^-$ (Fig. 6c). $(Na^+ + K^+)–Cl^-$ represents the amount by chloride salts dissolution (mostly halite dissolution), while $(Mg^{2+}+ Ca^{2+})–(SO_4^{2-} + HCO_3^-)$ represents the amount of Mg^{2+}+ Ca^{2+} gained or lost relative to that provided by gypsum, calcite and dolomite dissolution. If cation exchange is an important process that controls the ionic composition of the groundwater, the relationship between these parameters should be linear with a slope of −1 (Jalali 2007). Figure 6c indicates an increase in Na^++ K^+ with a decrease in Mg^{2+}+ Ca^{2+} or an increase in $SO_4^{2-} + HCO_3^-$. The fitted linear regression line has a slope of −0.89 ($R^2 = 0.65$), which clearly suggests the existence of cation exchange. In unconsolidated sediments of an aquifer system, there is always a considerable amount of clay minerals that can participate in the cation exchange reaction. Meanwhile, both CAI 1 and CAI 2 (Fig. 6d) are positive, also indicating that reverse ion exchange reactions take place and play an important role in hydrogeochemical evolution of groundwater.

Another significant characteristic of the groundwater in the Tashi sub-basin was the relative low NO_3^-. Approximately 70 % of samples had concentrations of less than 1 mg/L and most of them were collected from springs. In the Guazhou sub-basin, the NO_3^- concentrations range from 0.72 to 11.75 mg/L. This indicates that the quality of the groundwater is generally good and anthropogenic input to the groundwater system may be negligible.

Conceptual model of recharge source and hydrogeochemical evolution

Based on the isotopic and hydrogeochemical analysis, a conceptual model of groundwater recharge and hydrogeochemical evolution was developed to help understand groundwater circulation in the study area.

In the Tashi sub-basin, the snow and ice-melt water in the Qilian Mountains is the primary recharge source of groundwater (Fig. 7). The groundwater flows from south to north through this sub-basin. Dissolution is the control factor of hydrogeochemial evolution in this process, so the most evident features are that Mg^{2+}, Na^+, and Cl^- concentrations correlate with TDS with R^2 close to 1 and the TDS gradually increases along the groundwater flow direction. Meanwhile, the Mg^{2+}+ Ca^{2+} versus SO_4^{2-} + HCO_3^- also shows a good linear relationship and follows the expected 1:1 stoichiometry ratio. Similar to most arid regions of the world, along the groundwater flow direction, the overall chemistry of the anion facies in the water types changed from HCO_3^--dominated to SO_4^{2-}-dominated anions, and then to Cl^- dominated.

In the Guazhou sub-basin, most of the Shule River water from the Shuangta reservoir was used to irrigate farmland. Excess water drains straight down and infiltrates to recharge the underlying groundwater. This drainage is the main recharge source of the groundwater in the Guazhou sub-basin. The evidence is that the isotopic characteristics of the groundwater were very similar to those of the river water. Based on the statistical characteristics between various ions,

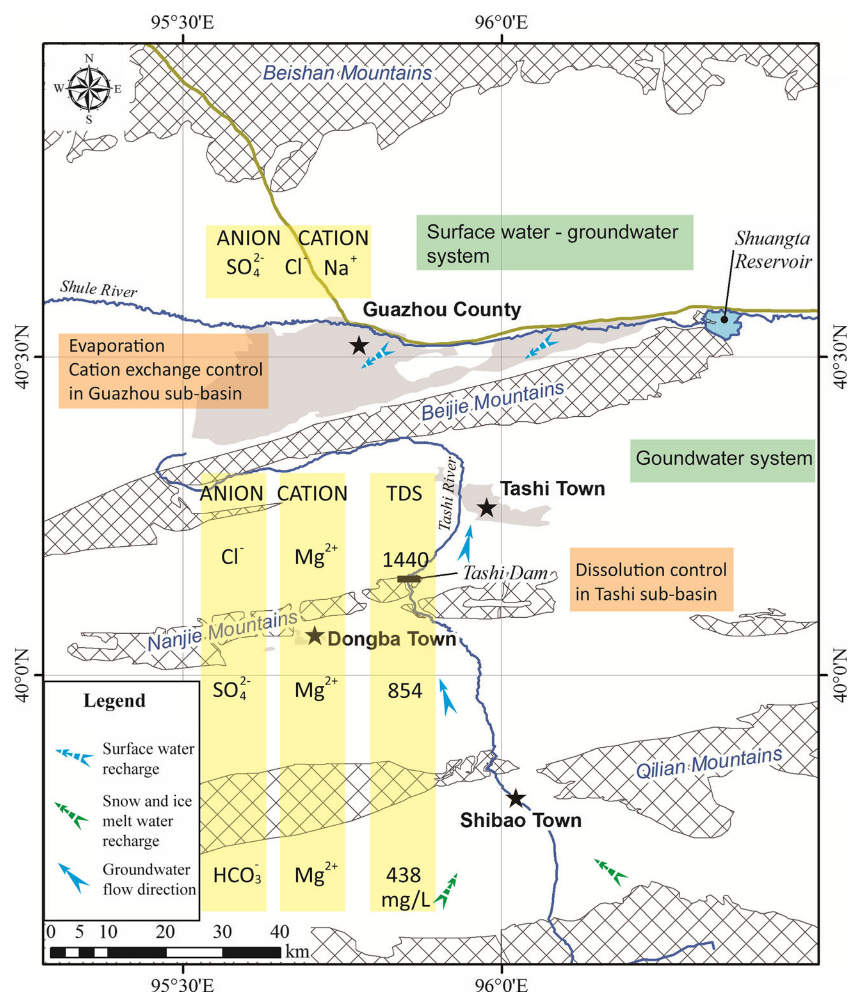

Fig. 7 Conceptual model of recharge sources and chemical processes leading to hydrogeochemical evolution of groundwater in the downstream section of Shule River Basin (*ANION* and *CATION* means dominant anion and dominant cation, respectively)

hydrogeochemical evolution of the groundwater is complex relative to that in the Tashi sub-basin, and includes cation exchange, evaporation and dissolution.

Summary and conclusions

Groundwater has played a dominant role in long-term water resources for meeting domestic, ecological, agricultural and industrial needs in arid regions of the world, including northwestern China. Groundwater recharge is often the most important parameter for sustainable utilization of water resources in these areas. In the present study, isotopic and hydrogeochemical tracers were employed to identify the recharge sources and understand the geochemical evolution of groundwater in the downstream of Shule River, including the Tashi sub-basin and the Guazhou sub-basin.

The stable isotopes indicate that the groundwater recharge sources of the Tashi sub-basin and the Guazhou sub-basin are different. Compared to the samples collected in the Guazhou sub-basin, the samples collected in the Tashi sub-basin were characterized by significantly depleted stable isotopes. The main recharge source of groundwater in the Tashi sub-basin is the snow and ice-melt water from the Qilian Mountains. In contrast, close connection between the Shule River water and the groundwater in the Guazhou sub-basin was found because the δD and $\delta^{18}O$ of Guazhou groundwater are similar to that of Shule River water; therefore, the groundwater in the Guazhou sub-basin is mainly sourced from seepage of surface water.

In the Tashi sub-basin, the strong and significant linear relationships between Na^+ and Cl^- indicate that the dissolution of halite strongly controls the concentrations of theses ions. Groundwater was far below saturation for halite, so halite minerals in the aquifer can easily enter groundwater. The plot of Mg^{2+}+ Ca^{2+} versus $SO_4^{2-} + HCO_3^-$ shows a good linear relationship that followed the expected 1:1 stoichiometry ratio, suggesting that these ions were derived from a mixture of the dissolution of calcite, dolomite and gypsum; hence, dissolution of minerals is the dominant process during groundwater evolution in the Tashi sub-baisn. In the Guazhou sub-basin, a linear relationship was also found between Na^+ and Cl^- and the SI of halite was far below 0. These features are similar to those of groundwater from Tashi sub-basin. Another significant feature is that the plot of (Mg^{2+}+ Ca^{2+})–($SO_4^{2-} + HCO_3^-$) versus (Na^++ K^+)–Cl^- shows a good linear relationship with a slope of −0.89, and both CAI 1 and CAI 2 are positive. These suggest that the reverse ion exchange reaction may occur in groundwater. Apart from the dissolution, reverse ion exchange reactions also play an important role in hydrogeochemical evolution of groundwater in the Guazhou sub-basin.

The scientific results have important implications for groundwater management in the downstream reach of Shule River. The recharge source of groundwater in the Tashi sub-basin is relatively abundant but it cannot flow laterally into the Guazhou sub-basin. As an important and major irrigation area in Hexi Corridor, sustainable and rational use of water resources is very important, especially in the Guazhou sub-basin where groundwater is mainly recharged from seepage of surface water. Most of the Shule River water has been impounded in order to regulate water for irrigation. The recharge amount of groundwater in the Guazhou sub-basin has reduced from 5.21×10^8 m^3/year to 2.86×10^8 m^3/year in the past 50 years (Yan 2007); therefore, the surface water should be used efficiently and routinely, while the groundwater exploitation should be limited as much as possible.

Acknowledgements This research was supported by the Youth Innovation Promotion Association Chinese Academy Sciences (Grant No. 2016063) and the Project funded by China Postdoctoral Science Foundation (Grant No. 2016 M591247). We are grateful to Dr. Martin Appold and the anonymous reviewers for their constructive comments and suggestions which greatly improved the manuscript.

References

Chen J, Liu X, Sun X, Su Z, Yong B (2014) The origin of groundwater in Zhangye Basin, northwestern China, using isotopic signature. Hydrogeol J 22(2):411–424. doi:10.1007/s10040-013-1051-7

Cloutier V, Lefebvre R, Savard MM, Bourque E, Therrien R (2006) Hydrogeochemistry and groundwater origin of the Basses-Laurentides sedimentary rock aquifer system, St. Lawrence lowlands, Quebec, Canada. Hydrogeol J 14(4):573–590. doi:10.1007/s10040-005-0002-3

Craig H (1961) Isotopic variations in meteoric waters. Science 133(3465):1702–1703

Currell MJ, Cartwright I (2011) Major-ion chemistry, delta C-13 and Sr-87/Sr-86 as indicators of hydrochemical evolution and sources of salinity in groundwater in the Yuncheng Basin, China. Hydrogeol J 19(4):835–850. doi:10.1007/s10040-011-0721-6

Dogramaci S, Skrzypek G (2015) Unravelling sources of solutes in groundwater of an ancient landscape in NW Australia using stable Sr, H and O isotopes. Chem Geol 393–394:67–78

Edmunds WM, Guendouz AH, Mamou A, Moulla A, Shand P, Zouari K (2003) Groundwater evolution in the Continental Intercalaire aquifer of southern Algeria and Tunisia: trace element and isotopic indicators. Appl Geochem 18(6):805–822

Edmunds WM, Ma JZ, Aeschbach-Hertig W, Kipfer R, Darbyshire DPF (2006) Groundwater recharge history and hydrogeochemical evolution in the Minqin Basin, North West China. Appl Geochem 21(12): 2148–2170

Eissa MA, Thomas JM, Pohll G, Hershey RL, Dahab KA, Dawoud MI, ElShiekh A, Gomaa MA (2013) Groundwater resource sustainability in the Wadi Watir delta, Gulf of Aqaba, Sinai, Egypt. Hydrogeol J 21(8):1833–1851. doi:10.1007/s10040-013-1031-y

Gansu Geology Survey (1978) The report and map for hydrogeological survey in the Changma, Anxi (1: 200,000). Gansu Science and Technology Press, Lanzhou, China

Girmay E, Ayenew T, Kebede S, Alene M, Wohnlich S, Wisotzky F (2015) Conceptual groundwater flow model of the Mekelle

Paleozoic–Mesozoic sedimentary outlier and surroundings (northern Ethiopia) using environmental isotopes and dissolved ions. Hydrogeol J 23(4):649–672. doi:10.1007/s10040-015-1243-4

Gonzalez-Ramon A, Rodriguez-Arevalo J, Martos-Rosillo S, Gollonet J (2013) Hydrogeological research on intensively exploited deep aquifers in the 'Loma de Aebeda' area (Jaén, southern Spain). Hydrogeol J 21(4):887–903. doi:10.1007/s10040-013-0957-4

Guendouz A, Moulla AS, Edmunds WM, Zouari K, Shand P, Mamou A (2003) Hydrogeochemical and isotopic evolution of water in the Complexe Terminal Aquifer in the Algerian Sahara. Hydrogeol J 11(4):483–495. doi:10.1007/s10040-003-0263-7

He JH, Ma JZ, Zhang P, Tian L, Zhu GF, Edmunds WM, Zhang Q (2012) Groundwater recharge environments and hydrogeochemical evolution in the Jiuquan Basin, Northwest China. Appl Geochem 27(4): 866–878. doi:10.1016/j.apgeochem.2012.01.014

He JH, Ma JZ, Zhao W, Sun S (2015) Groundwater evolution and recharge determination of the Quaternary aquifer in the Shule River basin, Northwest China. Hydrogeol J 23(8):1745–1759. doi:10.1007/s10040-015-1311-9

Herczeg AL, Leaney FW (2011) Review: environmental tracers in arid-zone hydrology. Hydrogeol J 19(1):17–29. doi:10.1007/s10040-010-0652-7

Herczeg AL, Dogramaci SS, Leaney FWJ (2001) Origin of dissolved salts in a large, semi-arid groundwater system: Murray Basin, Australia. Mar Freshw Res 52(1):41–52

Huang P, Wang Z (2010) Impact of human activity on groundwater recharge in Shule River basin, Northwest China. AGU Fall Meeting Abstracts 1:1057

IAEA, WMO (2004) Global network of isotopes in precipitation (GNIP) database. http://www.isohis.iaea.org. Accessed July 2016

Jalali M (2007) Salinization of groundwater in arid and semi-arid zones: an example from Tajarak, western Iran. Environ Geol 52(6):1133–1149

Ji X, Kang E, Chen R, Zhao W, Zhang Z, Jin B (2006) The impact of the development of water resources on environment in arid inland river basins of Hexi region, northwestern China. Environ Geol 50(6): 793–801. doi:10.1007/s00254-006-0251-z

Londono OMQ, Martinez DE, Dapena C, Massone H (2008) Hydrogeochemistry and isotope analyses used to determine groundwater recharge and flow in low-gradient catchments of the province of Buenos Aires, Argentina. Hydrogeol J 16(6):1113–1127. doi:10.1007/s10040-008-0289-y

Ma JZ, Wang XS, Edmunds WM (2005) The characteristics of groundwater resources and their changes under the impacts of human activity in the arid Northwest China: a case study of the Shiyang River Basin. J Arid Environ 61(2):277–295

Ma JZ, Pan F, Chen LH, Edmunds WM, Ding ZY, He JH, Zhou KP, Huang TM (2010) Isotopic and geochemical evidence of recharge sources and water quality in the Quaternary aquifer beneath Jinchang city, NW China. Appl Geochem 25(7):996–1007

Ma JZ, He JH, Qi S, Zhu GF, Zhao W, Edmunds WM, Zhao YP (2013) Groundwater recharge and evolution in the Dunhuang Basin, northwestern China. Appl Geochem 28(1):19–31

Martos-Rosillo S, Marin-Lechado C, Pedrera A, Vadillo I, Motyka J, Luis Molina J, Ortiz P, Martin Ramirez JM (2014) Methodology to evaluate the renewal period of carbonate aquifers: a key tool for their management in arid and semiarid regions, with the example of Becerrero aquifer, Spain. Hydrogeol J 22(3):679–689. doi:10.1007/s10040-013-1086-9

Montcoudiol N, Molson J, Lemieux JM, Cloutier V (2015) A conceptual model for groundwater flow and geochemical evolution in the southern Outaouais Region, Québec, Canada. Appl Geochem 58: 62–77. doi:10.1016/j.apgeochem.2015.03.007

Negrel P, Lemiere B, de Grammont HM, Billaud P, Sengupta B (2007) Hydrogeochemical processes, mixing and isotope tracing in hard rock aquifers and surface waters from the Subarnarekha River Basin, (east Singhbhum District, Jharkhand State, India). Hydrogeol J 15(8):1535–1552. doi:10.1007/s10040-007-0227-4

Parkhurst D, Appelo CAJ (1999) User's guide to PHREEQC (version 2): a computer program for speciation, reaction path, advective transport, and inverse geochemical calculation. US Geol Surv Water Resour Invest Rep 310:99–4259

Robertson WM, Sharp JM Jr (2013) Estimates of recharge in two arid basin aquifers: a model of spatially variable net infiltration and its implications (Red Light Draw and Eagle Flats, Texas, USA). Hydrogeol J 21(8):1853–1864. doi:10.1007/s10040-013-1018-8

Schoeller H (1965) Hydrodynamique dans le karst [Hydrodynamics of karst]. Actes du Colloques de Doubronik, IAHS/UNESCO, Wallingford, UK/Paris, pp 3–20

Sun ZY, Ma R, Wang YX, Hu YL, Sun LJ (2016) Hydrogeological and hydrogeochemical control of groundwater salinity in an arid inland basin: Dunhuang Basin, northwestern China. Hydrol Process 30(12):1884–1902. doi:10.1002/hyp.10760

Wang LH, Li GM, Dong YH, Han DM, Zhang JY (2015) Using hydrochemical and isotopic data to determine sources of recharge and groundwater evolution in an arid region: a case study in the upper–middle reaches of the Shule River basin, northwestern China. Environ Earth Sci 73(4):1–15. doi:10.1007/s12665-014-3719-2

Wang CX, Dong ZW, Qin X, Zhang J, Du WT, Wu JK (2016) Glacier meltwater runoff process analysis using δD and δ^{18}O isotope and chemistry at the remote Laohugou Glacier Basin in western Qilian Mountains, China. J Geogr Sci 26(6):722–734

Xi H, Feng Q, Si J, Chang Z, Cao S (2010) Impacts of river recharge on groundwater level and hydrochemistry in the lower reaches of Heihe River Watershed, northwestern China. Hydrogeol J 18(3):791–801. doi:10.1007/s10040-009-0562-8

Yan CY (2007) Study on the change of groundwater recharge and environment change caused by surface water redistribution (in Chinese). Arid Zone Res 24(04):428–433

Zhao LJ, Yin L, Xiao HL, Cheng GD, Zhou MX, Yang YG, Li CZ, Zhou J (2011) Isotopic evidence for the moisture origin and composition of surface runoff in the headwaters of the Heihe River basin. Chin Sci Bull 56(4–5):406–415. doi:10.1007/s11434-010-4278-x

Zhu GF, Su YH, Feng Q (2008) The hydrochemical characteristics and evolution of groundwater and surface water in the Heihe River Basin, northwest China. Hydrogeol J 16(1):167–182. doi:10.1007/s10040-007-0216-7